Compensating Random Transition-Detection Blackouts in Markov Networks

Alexander M. Maier, Benjamin Häsler, and Udo Seifert
II. Institut für Theoretische Physik, Universität Stuttgart, 70550 Stuttgart, Germany

(Received 7 November 2025; accepted 13 May 2026; published 16 June 2026)

In Markov networks, measurement blackouts with unknown frequency compromise observations such that thermodynamic quantities can no longer be inferred reliably. In particular, the observed currents neither discern equilibrium from nonequilibrium nor can they be used in extant estimators of entropy production. Our strategy to eliminate these effects is based on formally attributing the blackouts to a second channel connecting states. The unknown frequency of blackouts and the true underlying transition rates can be determined from the short-time limit of observed waiting-time distributions. A postmodification of observed trajectory data yields a virtual effective dynamics from which the lower bound on entropy production based on thermodynamic uncertainty relations can be recovered fully. Moreover, the postprocessed data can be used in waiting-time based estimators. Crucially, our strategy does not require the blackouts to occur homogeneously or symmetrically under time reversal.

DOI: 10.1103/p8yf-12yz

Introduction—Stochastic thermodynamics provides a comprehensive framework for the description and analysis of classical nonequilibrium systems on the nano- and microscale [1–5]. Its main assumption of an underlying stochastic Markovian dynamics is well verified experimentally for a huge class of systems ranging from electronic systems [6] to colloids [7] and simple biomolecules [8–10]. In more complex systems, however, not all of the relevant degrees of freedom participating in this underlying Markovian dynamics are experimentally accessible. At this point, the strategy of thermodynamic inference comes on stage aiming to extract information about thermodynamic quantities—with entropy production arguably being the most prominent one—from observations that explicitly or implicitly involve coarse graining over the underlying degrees of freedom [11,12].

Model-free lower bounds on entropy production can be based on the observation of transitions between lumped states [13–15], on evaluating the ratio of observed probabilities of forward and time-reversed coarse-grained trajectories [16–18], on the asymmetry of correlation functions [19–21], on measuring the statistics of certain rare events [22–25], on determining the displacement and force variances through the variance sum rule [26], on the measurement of currents and their variances through the thermodynamic uncertainty relation (TUR) [27–32] and its variants and refinements [33–52] or speed limits [53–58], and on the waiting-time distributions (WTDs) of observed transitions [59–71].

In essentially all of these techniques, a necessary requirement is that the observations are complete and error-free, the latter being a requirement recent works attempt to overcome [72–74]. Complete here means that once it is defined which (lumped) states, sequence of states, and transitions are "observable" in a given scheme, the observation will record completely whenever the system is in these states and undergoes the respective transitions. In other words, the observer does not encounter blackouts where the recording misses a state or a transition that is, in principle, observable.

Such blackouts are potentially devastating since they may mislead an observer even in the qualitative distinction between equilibrium and nonequilibrium. For a simple example, consider a three-state system where we can observe transitions through one of its links in the forward (+) and the backward (−) direction. If this observation is complete, then counting the frequency of + and − transitions suffices to distinguish equilibrium (same frequency) from nonequilibrium (a net current in one direction). If, however, we see only fractions η_+ and $\eta_- \neq \eta_+$ of the forward and the backward transitions, respectively, then we will falsely assign nonequilibrium even to an equilibrium system. Likewise, for a nonequilibrium system, we will measure a mean current and its variance that, if used naively in the TUR, may even overestimate the entropy production.

The purpose of this Letter is to introduce an approach that allows us to compensate for such unknown time-asymmetric random blackouts in the observation of transitions between the states of a Markov network. We will combine an analysis of the short-time limit of waiting-time

Published by the American Physical Society under the terms of the Creative Commons Attribution 4.0 International license. Further distribution of this work must maintain attribution to the author(s) and the published article's title, journal citation, and DOI.

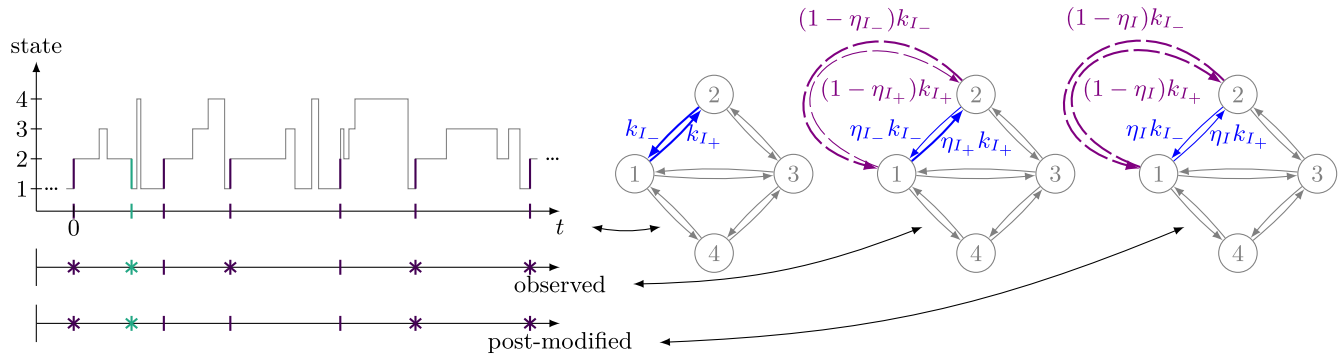


FIG. 1. Scheme of observation and postmodification. In the fluctuating microscopic trajectory (gray) of the left four-state Markov network only transitions $I_+ = (12)$ (indigo) and $I_- = (21)$ (green) with rates k_{I_+} and k_{I_-}, respectively, are, in principle, visible to an observer as indicated by the vertical bars. The actually observed transitions indicated by the crosses miss some of these bars due to random blackouts. The detection probabilities $\eta_{I_+} < 1$ and $\eta_{I_-} < 1$ lead to decreased effective rates $\eta_{I_+}k_{I_+}$ and $\eta_{I_-}k_{I_-}$ and to a second channel (purple) representing the blackouts with rates $(1-\eta_{I_+})k_{I_+}$ and $(1-\eta_{I_-})k_{I_-}$ as indicated in the middle network. The postmodification randomly discards transitions from the observed trajectory such that it corresponds to a virtual dynamics with equal detection probability for forward and backward transitions given by $\eta_I \leq \eta_I^* = \min\{\eta_{I_+}, \eta_{I_-}\}$ as indicated by the right network. Thus, observed transitions I_+ and I_- are discarded with probability η_I/η_{I_+} and η_I/η_{I_-}, respectively.

distributions between the observed transitions with postmodification of observed trajectories. This strategy allows us first to determine for each link the unknown fractions of blackouts $1-\eta_+$ and $1-\eta_-$ and to recover the true transition rates of this link. A subsequent postmodification of the trajectories yields thermodynamically consistent flowlike observables and combined with an analytical analysis of the TUR and the multidimensional TUR (MTUR) lets us recover the full value of the TUR ratio, and thus the lower bound on entropy production that we would have found in the absence of any blackouts. Finally, the waiting-time distributions based on the postprocessed data yield a lower bound on entropy production that can even be stronger than the full TUR.

Setup—We assume to observe one or more pairs of a transition and its reverse, which we call links, of a discrete-state Markov network. In particular, if a transition I_+ of some link $I = (I_+, I_-)$ occurs, we detect it with probability η_{I_+}. The same accounts for the corresponding transition I_- with η_{I_-}. This inability to detect all jumps along a trajectory renders observations incomplete as in the paradigmatic example shown in Fig. 1. The resulting observable dynamics is a renewal process for which the underlying Markov network effectively has two channels for each incompletely observable transition, e.g., a channel for transition $I_+ = (ij)$ from state i to j with rate $k_{I_+}\eta_{I_+}$ and one with $(1-\eta_{I_+})k_{I_+}$ as shown in Fig. 1. It is governed by observed, i.e., experimental, waiting-time distributions $\psi^{\mathrm{ex}}_{I_r\to J_s}(t)$. These provide the probability density for an observed trajectory that starts after transition I_r, with $r = +$ or $-$, of the link $I = (I_+, I_-)$ at time 0 and ends with the next observed transition J_s, with $s = +$ or $-$, of the link $J = (J_+, J_-)$ at time t. Whereas the distributions $\psi^{\mathrm{ex}}_{I_r\to J_s}(t)$ implicitly depend on the full set of detection probabilities $\boldsymbol{\eta} = \{\eta_{I_+}, \eta_{I_-}, \eta_{J_+}, \eta_{J_-}, \ldots\}$, the $\psi^{\mathrm{th}}_{I_r\to J_s}(t)$ for the theoretical case of perfect detection do not. Yet, the mean frequency $\nu^{\mathrm{ex}}_{I_r}$ of transitions I_r derived from the former differs only by a factor of η_{I_r} from its value in the latter case. Furthermore, for each type of superscript $\mathrm{ss} \in \{\mathrm{ex}, \mathrm{th}, \mathrm{pm}\ (\text{as introduced below})\}$, waiting-time distributions $\psi^{\mathrm{ss}}_{I_r\to J_s}(t)$ are normalized such that $\sum_{J_s}\int_0^\infty \psi^{\mathrm{ss}}_{I_r\to J_s}(t) = 1$, where J_s runs over all observable transitions including I_r.

Underlying the observable dynamics, we assume a discrete-state Markov network in its steady state. Transition rates $k_{ij} > 0$ for a jump from state i to j imply $k_{ji} > 0$ and generate the dynamics via the master equation

$$\partial_t p_i(t) = \sum_j [p_j(t)k_{ji} - p_i(t)k_{ij}] \equiv -\sum_j j_{ij}(t) \quad (1)$$

for the probability $p_i(t)$ of the system to be in state i at time t. If the system is in equilibrium, i.e., in detailed balance, all mean net currents j^s_{ij} vanish. Otherwise, the system is in a nonequilibrium steady state (NESS) with steady-state distribution p^s_i.

Inference of blackouts and restoring transition rates—The waiting-time distributions for consecutively observed transitions contain the topological information of how many hidden transitions are in the shortest path between the two observable ones [62,66]. In the short-time limit, WTDs are given by the probability density of such shortest path(s), i.e., a factor of t for each hidden transition multiplied with the product of rates along the respective path. For an incompletely observed link I with η_{I_+} and η_{I_-}, these paths contain no hidden transition between $I_+ = (ij)$ and $I_- = (ji)$ and one hidden transition in the sequences $I_+ \to I_+$ and $I_- \to I_-$, which, hence, leads to

$$\psi^{\mathrm{ex}}_{I_+\to I_+}(t) = (1-\eta_{I_-})k_{I_-}\eta_{I_+}k_{I_+}t + O(t^2), \tag{2}$$

$$\psi^{\mathrm{ex}}_{I_+\to I_-}(t) = \eta_{I_-}k_{I_-} + O(t), \tag{3}$$

$$\psi^{\mathrm{ex}}_{I_-\to I_+}(t) = \eta_{I_+}k_{I_+} + O(t), \tag{4}$$

$$\psi^{\mathrm{ex}}_{I_-\to I_-}(t) = (1-\eta_{I_+})k_{I_+}\eta_{I_-}k_{I_-}t + O(t^2). \tag{5}$$

In the short-time limit, the four equations (2)–(5) can be solved for the detection probability

$$\eta_{I_+} = \lim_{t\to 0}\frac{\psi^{\mathrm{ex}}_{I_-\to I_+}(t)}{\psi^{\mathrm{ex}}_{I_-\to I_+}(t) + \psi^{\mathrm{ex}}_{I_-\to I_-}(t)/t\psi^{\mathrm{ex}}_{I_+\to I_-}(t)} \tag{6}$$

and similarly for η_{I_-} by exchanging $+$ and $-$, and hence for the probabilities $1-\eta_{I_\pm}$ of a blackout and thereafter for the full rates $k_{I_+} = k_{ij}$ and $k_{I_-} = k_{ji}$. If all links of the network are observable and subject to random blackouts, this scheme yields all transition rates, i.e., the full generator, of the Markov network and hence access to the full dynamics. Using the steady-state probabilities, e.g., obtained as the eigenvector of the generator or by $p^s_i = \nu^{\mathrm{ex}}_{I_+}/\eta_{I_+}k_{I_+}$, enables us to check whether two states that are connected by an observable pair of transitions are in detailed balance, i.e., whether $j^s_{ij} = 0$. Hence, we can discern equilibrium from a NESS even if all transitions are subject to random blackouts of arbitrary unknown frequencies.

Even if, in contrast to all links as described in the last paragraph, only a few pairs of transitions are incompletely observable and others are hidden, this scheme allows us to infer the full set $\boldsymbol{\eta}$ and the rates of detectable transitions I_r as well as, based on their mean rates $\nu^{\mathrm{ex}}_{I_r}$, the steady-state probabilities of their adjacent states. Again, we can discern driven transitions and the ones with zero-mean net current and, if at least one link in each fundamental cycle is observable, effectively driven and undriven cycles.

Postmodifying trajectories—Knowing the full transition rates $k_{I_\pm}$ and the probabilities $\eta_{I_\pm}$ is insufficient for any inference technique based on higher moments than the mean of some flow, like for the TUR and for the entropy estimator based on waiting-time distributions, since these moments cannot be restored in general. Hence, we need to modify the statistics to achieve consistency between thermodynamic characteristics of the system and observables by removing the bias $\eta_{I_+} \neq \eta_{I_-}$ in all links I. Additionally, we use that thermodynamic inference allows for hidden links that we interpret here as the hidden second channel resulting from blackouts of an observable link; see Fig. 1. The goal of postmodifying the observed trajectory is to generate a trajectory of a virtual dynamics that is thermodynamically consistent and for which extant (thermodynamic) inference methods like the TUR estimator can be used. Indeed, if the relation $\eta_{I_+} = \eta_{I_-}$ held true for all I, then the blackouts could be considered as a thermodynamically consistent second unobserved channel between the corresponding states. The observations obtained for this particular set $\boldsymbol{\eta}$ could be used for inference of, e.g., a lower bound on the entropy production of the underlying Markov network by using the TUR. For the generic case of $\eta_{I_+} \neq \eta_{I_-}$, we identify $\eta^*_I \equiv \min\{\eta_{I_+}, \eta_{I_-}\}$. We can now randomly discard transitions in the observed trajectory such that the modified trajectory effectively corresponds to $\eta_{I_+} = \eta_{I_-} = \eta_I = \eta^*_I$ as illustrated in Fig. 1. In fact, we can thus generate trajectories for any $\eta_I \leq \eta^*_I$. The example in Fig. 2 shows the effect of postmodification on waiting-time distributions. These trajectories can, e.g., be used as input for both the TUR and the entropy estimator based on waiting-time distributions.

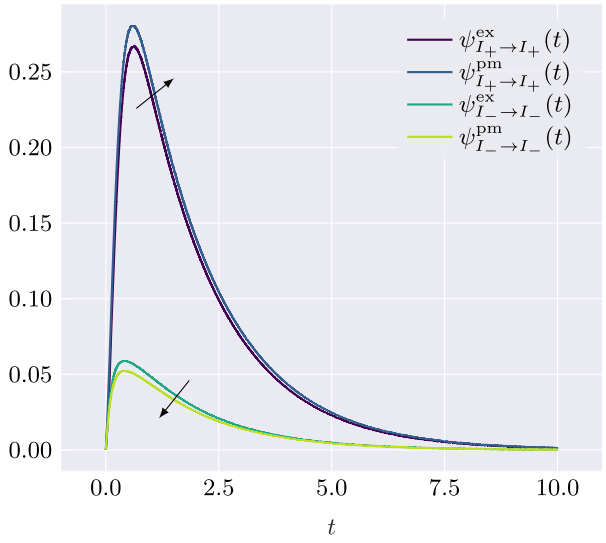


FIG. 2. Waiting-time distributions for one observable pair of transitions $I_+ = (12)$ and $I_- = (21)$ in the four-state Markov network from Fig. 1 with $k_{12} = k_{23} = 3$, $k_{31} = k_{14} = k_{43} = 2$, and $k_{13} = k_{21} = k_{32} = k_{34} = k_{41} = 1$ obtained via an analog of Gillespie's algorithm [75] for semi-Markov processes, see Methods in End Matter for details, with detection probabilities $\eta_{I_+} = 0.8$ and $\eta_{I_-} = 0.9$, trajectory length $T = 7\times 10^9$, bin width $\Delta t = 10^{-3}$, and cutoff time $t_c = 20$. The postmodification illustrated in Fig. 1 leads to the distributions for $\eta_I = 0.8$ as indicated by the arrows.

Entropy estimators—The mean entropy production rate [3–5]

$$\sigma_{\mathrm{M}} = \sum_{ij} p^s_i k_{ij} \ln\frac{k_{ij}}{k_{ji}} \tag{7}$$

is not directly accessible in Markov networks with hidden transitions and incomplete detections. However, estimators that remain valid for Markov networks with a hidden channel parallel to each observable link, like the TUR [36], yield nontrivial lower bounds of σ_{M}. The TUR,

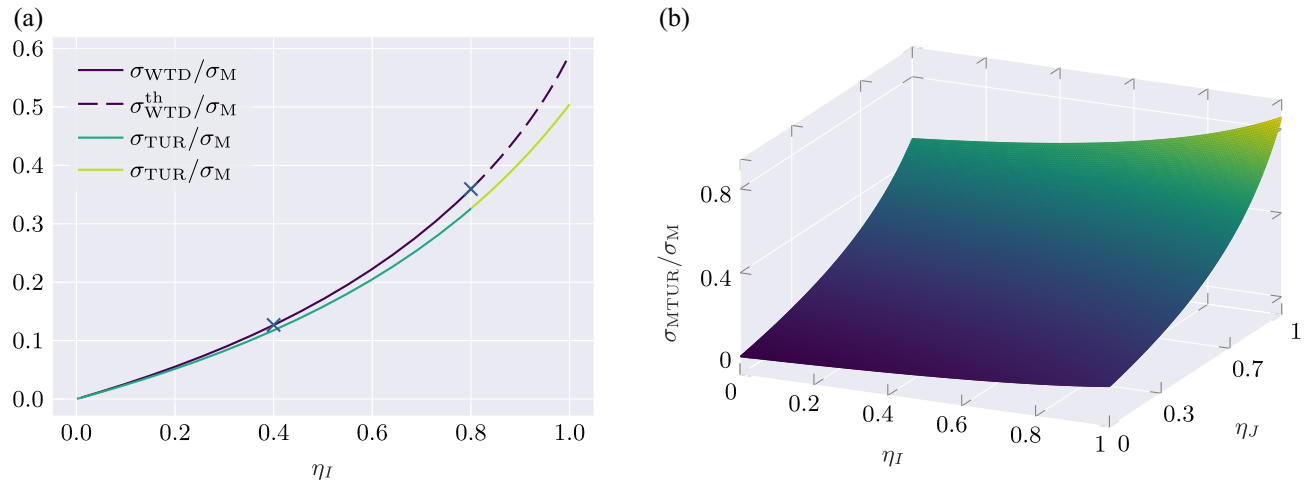


FIG. 3. Entropy estimators for observations with blackouts of the four-state Markov network from Fig. 1. (a) Entropy estimators $\sigma_{\mathrm{TUR}}(\eta_I)$ and $\sigma_{\mathrm{WTD}}(\eta_I)$ for the rates as given in the caption of Fig. 2 as a function of the detection probabilities $\eta_{I_+} = \eta_{I_-} = \eta_I$ in units of the mean entropy production rate σ_{M} of the underlying Markov network. The waiting-time distributions obtained from a simulated trajectory as presented in Fig. 2 result in the highlighted values of $\sigma_{\mathrm{WTD}}(\eta_I)$ (blue crosses). The uncertainty of these two values of η_I are not explicitly shown as the corresponding inferred values deviate by a few per mille from their theoretical value, e.g., $< 0.38\%$ for the right cross. The theoretical values of $\sigma_{\mathrm{WTD}}(\eta_I)$ for $\eta_I > \eta_I^* = 0.8$ (dashed) are inaccessible and require full knowledge of the system, whereas $\sigma_{\mathrm{TUR}}(\eta_I)$ can be inferred in this regime through Eq. (8) (green-yellow). (b) Entropy estimator $\sigma_{\mathrm{MTUR}}(\eta_I, \eta_J)$ as a function of the detection probabilities η_I and η_J in units of σ_{M} of this Markov network with rates $k_{12} = k_{23} = k_{31} = 2$, $k_{13} = k_{21} = k_{32} = k_{34} = k_{41} = 1$, and $k_{14} = k_{43} = 3$ in which, besides $I_+ = (12)$ and $I_- = (21)$, transitions $J_+ = (34)$ and $J_- = (43)$ are observable. See Methods in End Matter for more details on how these data have been generated.

$\sigma_{\mathrm{M}} \geq j^2/D \equiv \sigma_{\mathrm{TUR}}$ [27,28], for one link I is based on its mean current j_I^{pm} and the corresponding diffusion coefficient D_I^{pm}. In the presence of blackouts, the TUR estimator has the universal form

$$\sigma_{\mathrm{TUR}}(\eta_I) = (j_I^{\mathrm{pm}})^2/D_I^{\mathrm{pm}} = a\eta_I/(1 + b\eta_I) \tag{8}$$

with real constants a, b as argued below. It is thus sufficient to generate data for $\eta_I = \eta_I^*$ and, e.g., for $\eta_I = \eta_I^*/2$ to determine a and b. The numerical value $\sigma_{\mathrm{TUR}}(1) = a/(1 + b)$ then yields the value one would have determined if there were no blackouts.

The universal form of the TUR estimator (8) stems from the linear scaling of j_I^{pm} with η_I and from the intrinsic dynamical fluctuations and the binomial detection noise that lead to two effective terms of the diffusion coefficient D_I^{pm}, one is linear and one is quadratic in η_I. Theoretically, we find these dependencies by using the first cumulants extracted from the dominant eigenvalue $\lambda(z)$ of the tilted generator that generates the dynamics of the cumulant generating function [76], as detailed in End Matter.

For a general current based on multiple observable links $I, J, \ldots$, the TUR estimator takes the form

$$\sigma_{\mathrm{TUR}}(\boldsymbol{\eta}) = \frac{(\sum_I a_I \eta_I)^2}{\sum_I (b_I \eta_I + c_I \eta_I^2) + \sum_{I<J} d_{IJ} \eta_I \eta_J}, \tag{9}$$

where a_I, b_I, c_I, d_{IJ} are real and $I < J$ means that each unordered pair IJ contributes one term. In both cases, the post-modification allows us to determine the estimator σ_{TUR} for all $\boldsymbol{\eta}$, where $0 \leq \eta_I \leq \eta_I^*$ for each pair of transitions I_+, I_-. After determining its constants, i.e., the $a_{(I)}, b_{(I)}$, (c_I and d_{IJ}), by fitting its functional form (8) or (9), or the η dependence of the contributing cumulants, to the data, as described in End Matter, we can obtain the value of σ_{TUR} for any $\boldsymbol{\eta}$ including the ones with $\eta_I^* \leq \eta_I \leq 1$ for all I. Notably, we are therefore able to get σ_{TUR} as if we were able to register all transitions along observable transitions without blackouts, which we illustrate in Fig. 3(a).

The MTUR, which yields a tighter bound on σ_{M} than the TUR for a linear combination of observed currents by accounting for covariances [34], is still valid in our setup and can be analyzed analogously. For two pairs of observable transitions I_+, I_- and J_+, J_- with η_I and η_J, the explicit expression for σ_{MTUR} as a function of $\boldsymbol{\eta}$ becomes

$$\sigma_{\mathrm{MTUR}}(\eta_I, \eta_J) = \frac{a_1\eta_I + a_2\eta_J + a_3\eta_I\eta_J}{1 + a_4\eta_I + a_5\eta_J + a_6\eta_I\eta_J} \tag{10}$$

with real constants $a_l, l \in \{1, 2, \ldots, 6\}$ as detailed in End Matter. As for the TUR, after obtaining these constants from a fit, we can extend this estimator to get its value for $\boldsymbol{\eta} = \{1, 1, \ldots\}$ as if we were able to detect all jumps along

observable transitions. We illustrate the estimator (10) for a four-state network in Fig. 3(b).

Finally, in addition to the TURs, using waiting-time distributions obtained from our postmodification yields the entropy estimator

$$\sigma_{\mathrm{WTD}}(\boldsymbol{\eta}) = \sum_{r,s=\pm} \sum_{I,J} \int_0^\infty \nu_{I_r}^{\mathrm{pm}} \psi_{I_r \to J_s}^{\mathrm{pm}}(t) \ln \frac{\psi_{I_r \to J_s}^{\mathrm{pm}}(t)}{\psi_{\tilde{J}_s \to \tilde{I}_r}^{\mathrm{pm}}(t)} \mathrm{d}t \quad (11)$$

that follows from the one derived in Refs. [62,63] for complete blackout-free observations of Markov networks with only one pair of transitions between two adjacent states and with the tilde indicating the reversed transition. The estimator (11) constitutes a nontrivial lower bound of σ_{M} that depends on the full set $\boldsymbol{\eta}$ in a complex manner that includes infinite sums as the $\psi_{I_r \to J_s}^{\mathrm{pm}}(t)$ do. For an example, we show σ_{WTD}, which we have determined analytically and from a numerically simulated trajectory, in Fig. 3(a).

Concluding perspective—We have introduced a strategy to eliminate effects of random blackouts in the detection of transitions in Markov networks. By analyzing the short-time limit of the four waiting-time distributions associated with each link, both the unknown blackout rates and the true transition rates of this link can be inferred. In particular, a restored nonzero current through this link signifies nonequilibrium. If all transitions of a network are observable subject to blackouts with arbitrary unknown frequencies, the full dynamics can thus be restored. By postmodification of the trajectory data in partially observed networks, we can generate data that correspond to time-symmetric blackout rates and that are thermodynamically consistent with the underlying Markov network. Combined with the analytically derived dependence of the TUR bound on these blackout rates, this approach allows determination of the full bound even in the presence of arbitrary unknown blackouts. The same procedure works for the MTUR. Moreover, we have shown that a lower bound on entropy production derived from waiting-time distributions remains valid when using postmodified trajectories, despite time-asymmetric errors in the original data. The main results derived in this Letter have the status of proven theorems based, in principle, on infinite statistics. It will be important to address the impact of finite statistics including a quantification of uncertainties, arising, e.g., in the case of undersampling, in future works ideally in relation with specific experimental data.

The two main strategies introduced in this Letter—the recovery of blackout and transition rates and the post-modification of trajectory data based on the inferred blackout rates—are expected to be applicable beyond the stationary-state scenario discussed here. In particular, the same methodology could be extended to analyze blackouts in periodically and arbitrary time-dependently driven systems. Likewise, this approach of postprocessing trajectories should work in the inference of further thermodynamic quantities like cycle affinities [62,77], of topological information [71,78] and also beyond inequalities based on the TURs and the WTDs and beyond the assumption of time-reversal symmetric detection errors that could be described as spatial errors or faulty coarse graining [72–74]. Indeed, from a broader conceptual perspective, it is encouraging for future studies that we have learned here how to process data in which time-reversal symmetry is not only systematically broken—as it is in blackout-free observations of a non-equilibrium system—but additionally compromised in a random and inhomogeneous way.

Data availability—The data that support the findings of this article are not publicly available. The data are available from the authors upon reasonable request.

[1] K. Sekimoto, *Stochastic Energetics*, Lecture Notes in Physics (Springer, Berlin, Heidelberg, 2010).

[2] C. Jarzynski, Equalities and inequalities: Irreversibility and the second law of thermodynamics at the nanoscale, Annu. Rev. Condens. Matter Phys. **2**, 329 (2011).

[3] L. Peliti and S. Pigolotti, *Stochastic Thermodynamics. An Introduction* (Princeton University Press, Princeton, NJ, 2021).

[4] N. Shiraishi, *An Introduction to Stochastic Thermodynamics*, Fundamental Theories of Physics (Springer Nature Singapore, Singapore, 2023).

[5] U. Seifert, *Stochastic Thermodynamics* (Cambridge University Press, Cambridge, England, 2025).

[6] J. P. Pekola, Towards quantum thermodynamics in electronic circuits, Nat. Phys. **11**, 118 (2015).

[7] S. Ciliberto, Experiments in stochastic thermodynamics: Short history and perspectives, Phys. Rev. X **7**, 021051 (2017).

[8] A. Alemany, M. Ribezzi-Crivellari, and F. Ritort, From free energy measurements to thermodynamic inference in non-equilibrium small systems, New J. Phys. **17**, 075009 (2015).

[9] A. Kolomeisky, *Motor Proteins and Molecular Motors* (CRC Press, Boca Raton, 2015).

[10] F. S. Gnesotto, F. Mura, J. Gladrow, and C. P. Broedersz, Broken detailed balance and non-equilibrium dynamics in living systems: A review, Rep. Prog. Phys. **81**, 066601 (2018).

[11] U. Seifert, From stochastic thermodynamics to thermodynamic inference, Annu. Rev. Condens. Matter Phys. **10**, 171 (2019).

[12] C. Dieball and A. Godec, Perspective: Time irreversibility in systems observed at coarse resolution, J. Chem. Phys. **162**, 090901 (2025).

[13] M. Esposito, Stochastic thermodynamics under coarse graining, Phys. Rev. E **85**, 041125 (2012).

[14] S. Bo and A. Celani, Entropy production in stochastic systems with fast and slow time-scales, J. Stat. Phys. **154**, 1325 (2014).

[15] D. J. Skinner and J. Dunkel, Improved bounds on entropy production in living systems, Proc. Natl. Acad. Sci. U.S.A. **118**, e2024300118 (2021).

[16] R. Kawai, J. M. R. Parrondo, and C. Van den Broeck, Dissipation: The phase-space perspective, Phys. Rev. Lett. **98**, 080602 (2007).
[17] A. Gomez-Marin, J. M. R. Parrondo, and C. Van den Broeck, Lower bounds on dissipation upon coarse-graining, Phys. Rev. E **78**, 011107 (2008).
[18] E. Roldán and J. M. R. Parrondo, Estimating dissipation from single stationary trajectories, Phys. Rev. Lett. **105**, 150607 (2010).
[19] A. Dechant, J. Garnier-Brun, and S.-i. Sasa, Thermodynamic bounds on correlation times, Phys. Rev. Lett. **131**, 167101 (2023).
[20] C. Dieball and A. Godec, Thermodynamic correlation inequalities for finite times and transients, J. Phys. A **58**, 255001 (2025).
[21] T. Van Vu, V. T. Vo, and K. Saito, Dissipation, quantum coherence, and asymmetry of finite-time cross-correlations, Phys. Rev. Res. **6**, 013273 (2024).
[22] E. Roldán, I. Neri, M. Dörpinghaus, H. Meyr, and F. Jülicher, Decision making in the arrow of time, Phys. Rev. Lett. **115**, 250602 (2015).
[23] I. Neri, E. Roldán, and F. Jülicher, Statistics of infima and stopping times of entropy production and applications to active molecular processes, Phys. Rev. X **7**, 011019 (2017).
[24] S. Pigolotti, I. Neri, E. Roldán, and F. Jülicher, Generic properties of stochastic entropy production, Phys. Rev. Lett. **119**, 140604 (2017).
[25] I. Neri and M. Polettini, Extreme value statistics of edge currents in Markov jump processes and their use for entropy production estimation, SciPost Phys. **14**, 131 (2023).
[26] I. Di Terlizzi, M. Gironella, D. Herraez-Aguilar, T. Betz, F. Monroy, M. Baiesi, and F. Ritort, Variance sum rule for entropy production, Science **383**, 971 (2024).
[27] A. C. Barato and U. Seifert, Thermodynamic uncertainty relation for biomolecular processes, Phys. Rev. Lett. **114**, 158101 (2015).
[28] T. R. Gingrich, J. M. Horowitz, N. Perunov, and J. L. England, Dissipation bounds all steady-state current fluctuations, Phys. Rev. Lett. **116**, 120601 (2016).
[29] C. Hyeon and W. Hwang, Physical insight into the thermodynamic uncertainty relation using Brownian motion in tilted periodic potentials, Phys. Rev. E **96**, 012156 (2017).
[30] W. Hwang and C. Hyeon, Energetic costs, precision, and transport efficiency of molecular motors, J. Phys. Chem. Lett. **9**, 513 (2018).
[31] Y. Song and C. Hyeon, Thermodynamic uncertainty relation to assess biological processes, J. Chem. Phys. **154**, 130901 (2021).
[32] C. Maggi, F. Saglimbeni, V. C. Sosa, R. Di Leonardo, B. Nath, and A. Puglisi, Thermodynamic limits of sperm swimming precision, PRX Life **1**, 013003 (2023).
[33] K. Proesmans and C. van den Broeck, Discrete-time thermodynamic uncertainty relation, Europhys. Lett. **119**, 20001 (2017).
[34] A. Dechant, Multidimensional thermodynamic uncertainty relations, J. Phys. A **52**, 035001 (2018).
[35] D. M. Busiello and S. Pigolotti, Hyperaccurate currents in stochastic thermodynamics, Phys. Rev. E **100**, 060102(R) (2019).
[36] K. Liu, Z. Gong, and M. Ueda, Thermodynamic uncertainty relation for arbitrary initial states, Phys. Rev. Lett. **125**, 140602 (2020).
[37] J. M. Horowitz and T. R. Gingrich, Thermodynamic uncertainty relations constrain non-equilibrium fluctuations, Nat. Phys. **16**, 15 (2020).
[38] T. Koyuk and U. Seifert, Thermodynamic uncertainty relation for time-dependent driving, Phys. Rev. Lett. **125**, 260604 (2020).
[39] A. Dechant and S.-i. Sasa, Fluctuation–response inequality out of equilibrium, Proc. Natl. Acad. Sci. U.S.A. **117**, 6430 (2020).
[40] A. Dechant and S.-i. Sasa, Continuous time reversal and equality in the thermodynamic uncertainty relation, Phys. Rev. Res. **3**, L042012 (2021).
[41] S. K. Manikandan, D. Gupta, and S. Krishnamurthy, Inferring entropy production from short experiments, Phys. Rev. Lett. **124**, 120603 (2020).
[42] S. Otsubo, S. Ito, A. Dechant, and T. Sagawa, Estimating entropy production by machine learning of short-time fluctuating currents, Phys. Rev. E **101**, 062106 (2020).
[43] T. Van Vu, V. T. Vo, and Y. Hasegawa, Entropy production estimation with optimal current, Phys. Rev. E **101**, 042138 (2020).
[44] A. Dechant and S. I. Sasa, Improving thermodynamic bounds using correlations, Phys. Rev. X **11**, 041061 (2021).
[45] E. Roldán, J. Barral, P. Martin, J. M. R. Parrondo, and F. Jülicher, Quantifying entropy production in active fluctuations of the hair-cell bundle from time irreversibility and uncertainty relations, New J. Phys. **23**, 083013 (2021).
[46] S. Otsubo, S. K. Manikandan, T. Sagawa, and S. Krishnamurthy, Estimating time-dependent entropy production from non-equilibrium trajectories, Commun. Phys. **5**, 11 (2022).
[47] C. Dieball and A. Godec, Direct route to thermodynamic uncertainty relations and their saturation, Phys. Rev. Lett. **130**, 087101 (2023).
[48] T. Van Vu and K. Saito, Thermodynamic unification of optimal transport: Thermodynamic uncertainty relation, minimum dissipation, and thermodynamic speed limits, Phys. Rev. X **13**, 011013 (2023).
[49] P. Pietzonka and F. Coghi, Thermodynamic cost for precision of general counting observables, Phys. Rev. E **109**, 064128 (2024).
[50] S. K. Manikandan, T. Ghosh, T. Mandal, A. Biswas, B. Sinha, and D. Mitra, Estimate of entropy production rate can spatiotemporally resolve the active nature of cell flickering, Phys. Rev. Res. **6**, 023310 (2024).
[51] T. Aslyamov, K. Ptaszyński, and M. Esposito, Nonequilibrium fluctuation-response relations: From identities to bounds, Phys. Rev. Lett. **134**, 157101 (2025).
[52] T. Indo and Y. Hasegawa, Thermodynamic uncertainty relation for generalized time-reversal observables, arXiv:2509.01981.
[53] K. Yoshimura and S. Ito, Thermodynamic uncertainty relation and thermodynamic speed limit in deterministic chemical reaction networks, Phys. Rev. Lett. **127**, 160601 (2021).
[54] S. Ito, Stochastic thermodynamic interpretation of information geometry, Phys. Rev. Lett. **121**, 030605 (2018).

[55] N. Shiraishi, K. Funo, and K. Saito, Speed limit for classical stochastic processes, Phys. Rev. Lett. **121**, 070601 (2018).
[56] V. T. Vo, T. Van Vu, and Y. Hasegawa, Unified approach to classical speed limit and thermodynamic uncertainty relation, Phys. Rev. E **102**, 062132 (2020).
[57] G. Falasco and M. Esposito, Dissipation-time uncertainty relation, Phys. Rev. Lett. **125**, 120604 (2020).
[58] S. Ito and A. Dechant, Stochastic time evolution, information geometry, and the Cramér-Rao bound, Phys. Rev. X **10**, 021056 (2020).
[59] I. A. Martínez, G. Bisker, J. M. Horowitz, and J. M. R. Parrondo, Inferring broken detailed balance in the absence of observable currents, Nat. Commun. **10**, 3542 (2019).
[60] D. J. Skinner and J. Dunkel, Estimating entropy production from waiting time distributions, Phys. Rev. Lett. **127**, 198101 (2021).
[61] J. Ehrich, Tightest bound on hidden entropy production from partially observed dynamics, J. Stat. Mech. (2021) 083214.
[62] J. van der Meer, B. Ertel, and U. Seifert, Thermodynamic inference in partially accessible Markov networks: A unifying perspective from transition-based waiting time distributions, Phys. Rev. X **12**, 031025 (2022).
[63] P. E. Harunari, A. Dutta, M. Polettini, and E. Roldan, What to learn from a few visible transitions' statistics?, Phys. Rev. X **12**, 041026 (2022).
[64] J. van der Meer, J. Degünther, and U. Seifert, Time-resolved statistics of snippets as general framework for model-free entropy estimators, Phys. Rev. Lett. **130**, 257101 (2023).
[65] K. Blom, K. Song, E. Vouga, A. Godec, and D. E. Makarov, Milestoning estimators of dissipation in systems observed at a coarse resolution, Proc. Natl. Acad. Sci. U.S.A. **121**, e2318333121 (2024).
[66] A. M. Maier, J. Degünther, J. van der Meer, and U. Seifert, Inferring kinetics and entropy production from observable transitions in partially accessible, periodically driven Markov networks, J. Stat. Phys. **191**, 104 (2024).
[67] P. E. Harunari, C. E. Fiore, and A. C. Barato, Inference of entropy production for periodically driven systems, Phys. Rev. E **110**, 064126 (2024).
[68] U. Kapustin, A. Ghosal, and G. Bisker, Utilizing time-series measurements for entropy-production estimation in partially observed systems, Phys. Rev. Res. **6**, 023039 (2024).
[69] B. Ertel and U. Seifert, Estimator of entropy production for partially accessible Markov networks based on the observation of blurred transitions, Phys. Rev. E **109**, 054109 (2024).
[70] J. Degünther, J. van der Meer, and U. Seifert, General theory for localizing the where and when of entropy production meets single-molecule experiments, Proc. Natl. Acad. Sci. U.S.A. **121**, e2405371121 (2024).
[71] A. M. Maier, U. Seifert, and J. van der Meer, From observed transitions to hidden paths in Markov networks, Phys. Rev. Res. **7**, 033067 (2025).
[72] M. Ferri-Cortes, J. A. Almanzaa-Marrero, R. Lopez, R. Zambrini, and G. Manzano, Conditional fluctuation theorems and entropy production for monitored quantum systems under imperfect detection, Phys. Rev. Res. **7**, 013077 (2025).
[73] J. van der Meer and K. Saito, Thermodynamic bounds and error correction for faulty coarse graining, Phys. Rev. Res. **7**, 043260 (2025).
[74] R. Bao, N. Ohga, and S. Ito, Measuring irreversibility by counting: A random coarse-graining framework, arXiv:2508.11586.
[75] D. T. Gillespie, Exact stochastic simulation of coupled chemical reactions, J. Phys. Chem. **81**, 2340 (1977).
[76] Z. Koza, General technique of calculating the drift velocity and diffusion coefficient in arbitrary periodic systems, J. Phys. A **32**, 7637 (1999).
[77] N. Ohga, S. Ito, and A. Kolchinsky, Thermodynamic bound on the asymmetry of cross-correlations, Phys. Rev. Lett. **131**, 077101 (2023).
[78] X. Zhao, D. E. Makarov, and A. Godec, Towards Markov-state holography, New J. Phys. **27**, 125002 (2025).
[79] K. Sekimoto, Derivation of the first passage time distribution for Markovian process on discrete network, arXiv:2110.02216.

End Matter

Tilted-generator approach to cumulants—Cumulants of an arbitrary integrated current, e.g., the net count of transitions through a link, are determined by their cumulant generating function or its scaled version. The latter is the largest (dominant) eigenvalue, $\lambda(z)$, of the tilted generator $\boldsymbol{L}(z)$ that rules the time evolution of the so-called end-state resolved moment generating function of a trajectory with length $T \to \infty$, see, e.g., Ref. [5]. The elements of this generator are given by

$$\boldsymbol{L}_{ij}(z) = k_{ji} e^{z d_{ji}} - \delta_{ij} \sum_l k_{il}, \tag{A1}$$

where the nonvanishing $d_{ij} = -d_{ji}$ is the asymmetric increment of transitions from state i to j contributing to the current of interest and δ_{ij} is the Kronecker delta. In the limit $z \to 0$, the nth derivative of the largest eigenvalue $\lambda(z)$ of this operator then leads to the nth cumulant of the fluctuating current $\hat{j}$,

$$\mathcal{C}_n(\hat{j}) = T^{1-n} \partial_z \lambda(z)_{|z=0}. \tag{A2}$$

A more direct route than finding $\lambda(z)$ and taking its derivatives uses $\lambda(0) = 0$ in derivatives of the characteristic polynomial

$$\chi(z) = \det\{\boldsymbol{L}(z) - \lambda \mathbf{1}\} \equiv \sum_{i=0}^{d} c_i(z) \lambda^i(z) = 0, \tag{A3}$$

where the unit matrix $\mathbf{1}$ and $\boldsymbol{L}(z)$ have d rows and the last equality enforces $\lambda(z)$ to be an eigenvalue.

This approach is iterative leading to the first two cumulants,

$$j \equiv \langle \hat{j} \rangle = -c_0'/c_{1|z=0} \quad \text{and} \tag{A4}$$

$$D_{\hat{j}} = \mathrm{Var}(\hat{j})T/2 = -(c_0'' + 2c_1' j + 2c_2 j^2)/2c_{1|z=0}, \tag{A5}$$

where primes indicate derivatives ∂_z and we have dropped the z dependencies.

Blackouts modify the elements of the tilted generator to

$$\boldsymbol{L}_{ij}(z) = k_{ji}(\eta_{ji} e^{z d_{ji}} + 1 - \eta_{ji}) - \delta_{ij} \sum_l k_{il}. \tag{A6}$$

For the virtual dynamics after postmodification, we have $\eta_{ij} = 0$ for hidden transitions and $\eta_{ij} = \eta_{ji}$ otherwise. The functions $c_i(z)$ in the characteristic polynomial (A3) then depend on the full vector of detection probabilities $\boldsymbol{\eta}$. In particular, they consist of terms with factors of the form $k_{ji}(\eta_{ji} e^{z d_{ji}} + 1 - \eta_{ji})$, which reduce to k_{ji} for $z = 0$. Hence, all first derivatives $c_i'(0)$ either vanish or are linear in the elements of $\boldsymbol{\eta}$. Moreover, second derivatives $c_i''(0)$ either vanish or consist of linear terms in at least some η_{ij} as well as of terms that are quadratic or bilinear in elements of $\boldsymbol{\eta}$. This pattern continues for higher derivatives $c_i^{(n)}(0)$ as a direct consequence of the derivative of products until n equals the largest degree of $c_i(z)$ in $\boldsymbol{\eta}$. Derivatives $c_i^{(m)}(0)$ with $m > n$ meet the same criteria as the $c_i^{(n)}(0)$. Using these insights, we find that the mean current (A4) is linear in all elements of $\boldsymbol{\eta}$ as one would intuitively expect, i.e.,

$$j^{\mathrm{pm}} = \sum_I a_I \eta_I \quad \text{with real constants } a_I. \tag{A7}$$

The diffusion coefficient (A5) then becomes

$$D_{\hat{j}}^{\mathrm{pm}} = \sum_I (b_I \eta_I + c_I \eta_I^2) + \sum_{I<J} d_{IJ} \eta_I \eta_J, \tag{A8}$$

where b_I, c_I, and d_{IJ} are real constants. We have simplified the notation by using the concept of links $I = (I_+, I_-)$ introduced in the main text because any pair $ij = I_+$ and $ji = I_-$ has $\eta_{I_+} = \eta_{I_-} = \eta_I$. Based on the insights about $c_i^{(n)}(0)$ and the determination of higher derivatives of $\lambda(z)$ making use of lower-order cumulants or, equivalently, of the lower-order derivatives of $\lambda(z)$ like the ones in Eqs. (A4) and (A5), the nth cumulant must be a polynomial in the detection probabilities of degree n without constant term.

The above analysis for the case with blackouts generalizes readily to the case of multiple fluctuating currents. In this case, we introduce a vector $\boldsymbol{z}$ with one element per fluctuating current. The tilted generator (A6) and its characteristic polynomial are, hence, modified such that the exponential functions scale each transition rate only by the element of $\boldsymbol{z}$ corresponding to the same fluctuating current. Then, cumulants of a single current result as above and mixed derivatives like $\partial_{z_1}\partial_{z_2}\lambda(\boldsymbol{z})|_{\boldsymbol{z}=0}$ yield joint cumulants of two or more fluctuating currents. In the case of two fluctuating currents, the cumulants so found yield the entropy estimator of the MTUR (10).

Fitting cumulants or entropy estimators to data—The constants $a_{(I)}, b_{(I)}$, (c_I and d_{IJ}) in Eqs. (8)–(10) can be obtained in various ways by fitting the functional form of these equations to measurement data. While arbitrarily elaborate fitting algorithms, or in the case of Eq. (9) a smart choice of $\boldsymbol{\eta}$ simplifying quadrics, yield the constants, we present here a simpler route. Using n estimator values of distinct $\boldsymbol{\eta}$ for the n constants in Eqs. (8) and (10) provides a system of linear equations. Solving it determines the sought constants. While a similar approach can be adapted to Eq. (9) too, there is an even simpler procedure, which works for all three estimators (8)–(10). This procedure uses the dependence of cumulants of a fluctuating current on $\boldsymbol{\eta}$ derived above since the estimators are a function of these cumulants. Determining the constants in the expression of an estimator, hence, reduces to finding their value in the respective cumulants. Importantly, these cumulants are linear in these constants and each set of data yielding one estimator value yields one value for the mean current (A7) and for the diffusion coefficient (A8). Hence, solving the system of linear equations for both the mean current and the diffusion coefficient leads to all needed constants.

Methods for Figs. 2 and 3—The WTDs shown in Fig. 2 have been determined using an analog of Gillespie's algorithm for semi-Markov processes since the observed dynamics consisting of transitions and waiting times in between can be seen as a semi-Markov process with transitions figuring as states. Like in Gillespie's algorithm the next observable transition and the waiting time since the last observed transition are each fixed by a randomly drawn number, which is uniformly distributed in $[0, 1)$, based on analytically determined cumulative WTDs. These cumulative WTDs result by integration from the WTDs, which are obtained by solving the absorbing master equation of the Markov network resulting from rerouting observable transitions (channels) into auxiliary states [62,79]. Since sampling infinitely many bins is impossible in finite time, we discard any transition with waiting time longer than the cutoff time t_c, i.e., we determine the binned WTDs only in the interval $[0, t_c]$, where t_c is large enough so that the true WTDs obtained via the absorbing network are negligibly small beyond this time.

Besides data obtained from such a Gillespie-like simulation, Fig. 3 contains analytically determined data. First, unless stated otherwise, WTDs have been determined using

the analytical method described above. Second, cumulants of one or multiple observed fluctuating currents needed for the TUR or the MTUR, respectively, have been determined analytically using the formalism based on the tilted generator, which we describe above. Third, the entropy production rate (7) of the underlying Markov network has been calculated using the transition rates and the steady-state distribution, determined as the eigenvector associated with eigenvalue zero, of the master equation (1).